

Figure S1, related to Figure 1, Differentiation and Characterization of Patient-Specific iPS cell-derived Motor Neurons. (A) Schematic of differentiation protocol (see methods for details). (B-C) Differentiations typically yielded neurons that expressed TUJ1, the MN transcription factors ISL and HB9, as well as MAP2. Many ISL+ MNs were FOXP1^{high} and all were HOXA5⁺ indicating their acquisition of a lateral motor column identity with a rostral phenotype, at 30 days post-dissociation, ISL+ MNs were ChAT-positive. (D-G) *Hb9*::RFP positive MNs are electrophysiologically active. RFP+ cells show a 6-fold enrichment in *Hb9* expression levels than the RFP negative fraction. In whole-cell patch clamping recordings of day 15 neurons in co-culture with glia, MNs exhibited initial inward sodium currents followed by outward potassium currents upon depolarization in voltage-clamp mode, as well as repetitive action potential firing in current-clamp mode, as well as kainate and GABA responses (all scale bars=50 μ m).

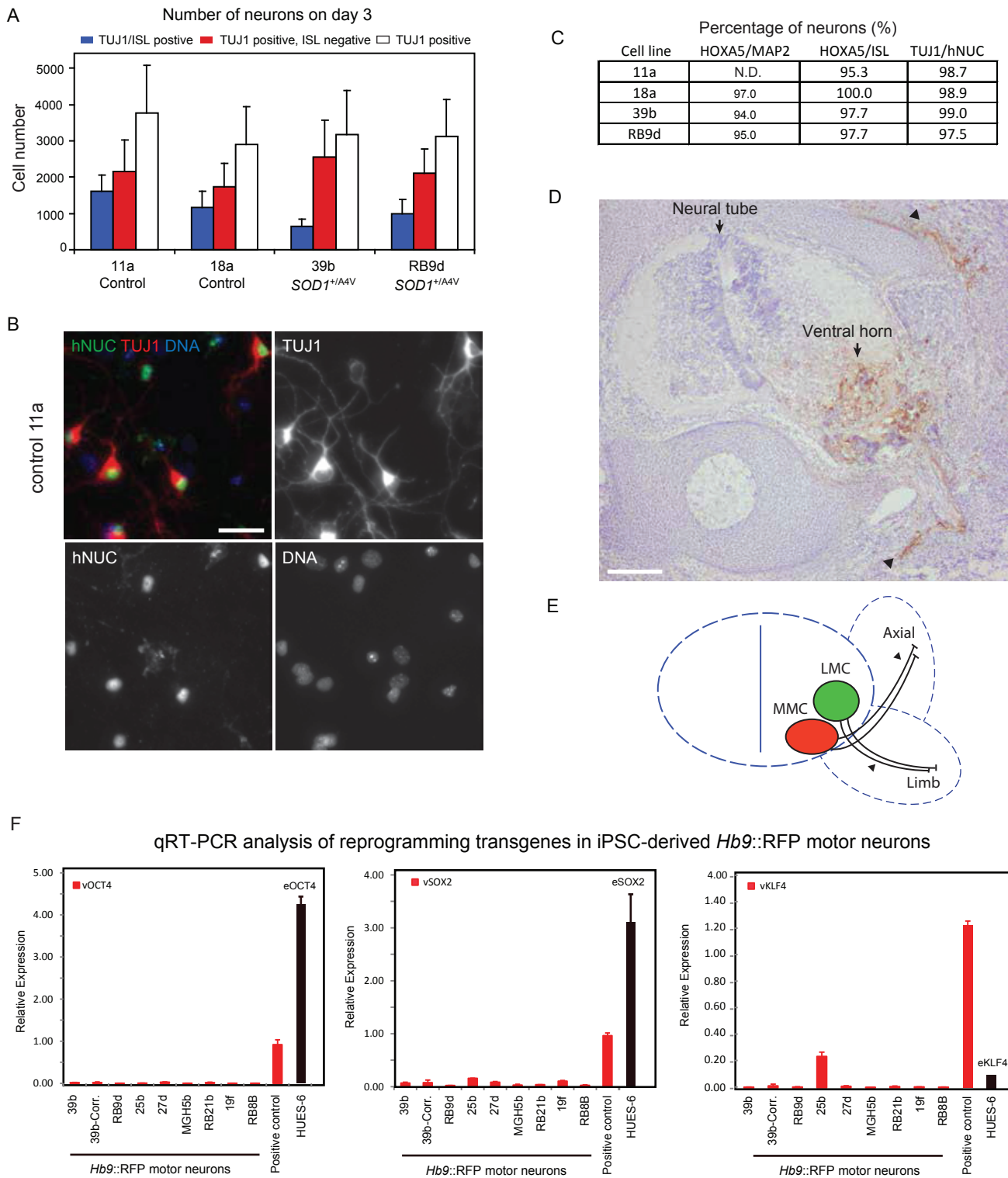


Figure S2, related to Figure 1, Characterization of Patient-Specific iPSC cell-derived Motor Neurons. (A) Quantifications of efficiencies of differentiation for each of the 4 iPSC cell lines. **(B)** More than 97% of TUJ1+ve neurons are iPSC-derived as they stain positive for the human nuclear antigen (hNUC). **(C)** Quantifications of HOXA5 and human (hNUC) MNs and neurons. N.D.: Not determined. **(D)** Transplantation of *Hb9*::GFP+ MNs into chick embryo spinal cords showed MNs settling into the ventral root and extending axons (black arrow heads) towards the axial and limb musculature. **(E)** Graphic representation of panel J, black arrow heads match MN axons from (D), MMC: Median motor column, LMC: Lateral motor column. **(F)** Transgene expression in *Hb9*::RFP purified MNs. Endogenous levels of *OCT4*, *SOX2* and *KLF4* in HUES-6 ES cells are shown for comparison. An iPSC line that shows residual expression of the reprogramming transgenes was used as a positive control.

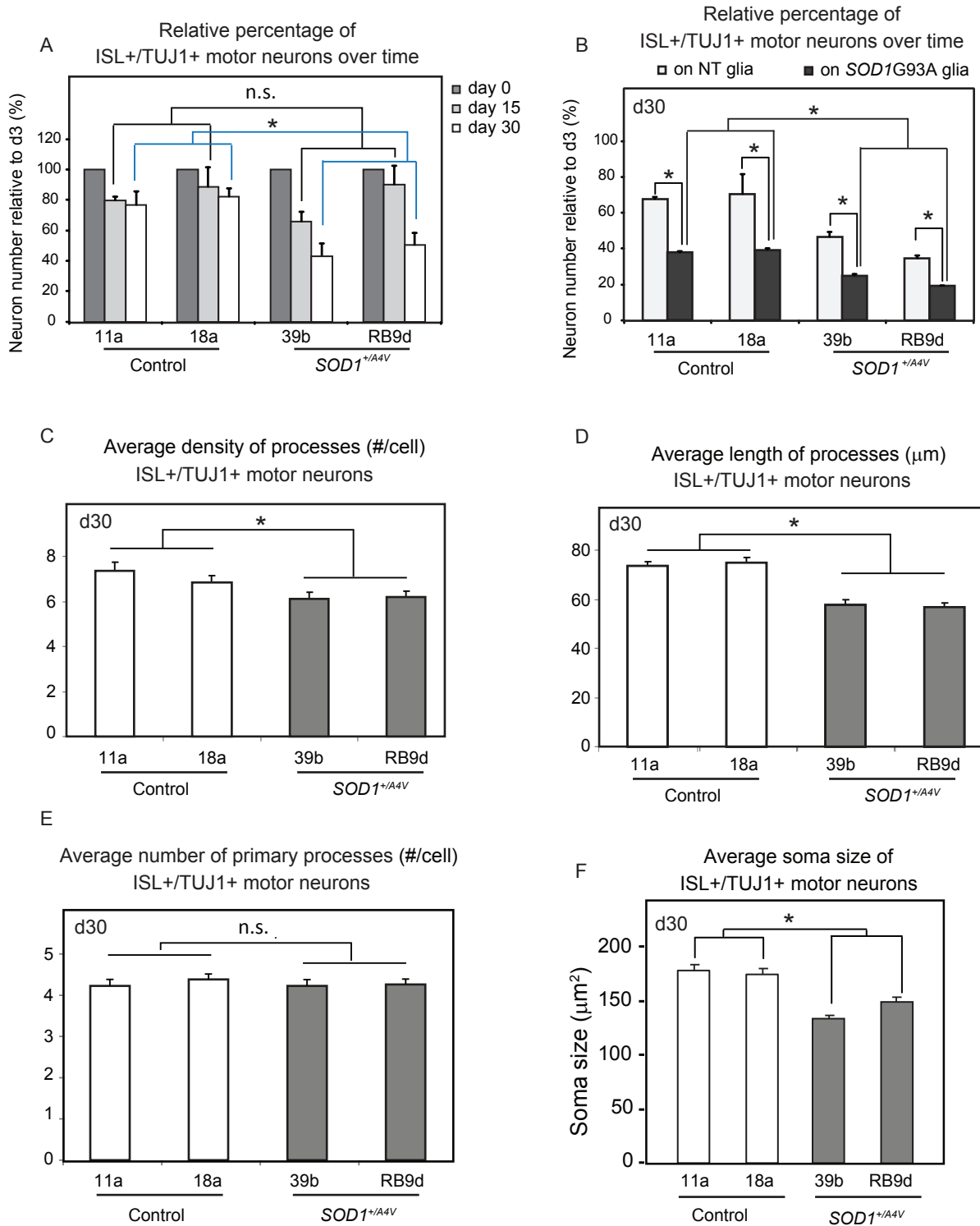


Figure S3, related to Figure 1, Survival and Morphological Alterations of *SOD1*^{+/A4V} MNs. (A) *SOD1*^{+/A4V} MNs exhibit reduced survival over time in culture (n=3, +/-SEM, P<0.05). (B) MNs are sensitive to the toxic effects of primary glia from *SOD1*^{G93A} mice. (C) Quantifications of MN processes, evaluated as total number of TUJ1+ve processes per cell showed that *SOD1*^{+/A4V} MNs are less elaborate after 30 days in culture; (D) and have shorter processes (n=3, +/-SEM, P<0.05), (E) but not fewer primary processes. (F) Soma size of ISL+/TUJ1+ MNs (μm²) measured at day 30. *SOD1*^{+/A4V} MNs exhibit reduced size than controls (n=3, +/-SEM, P<0.05).

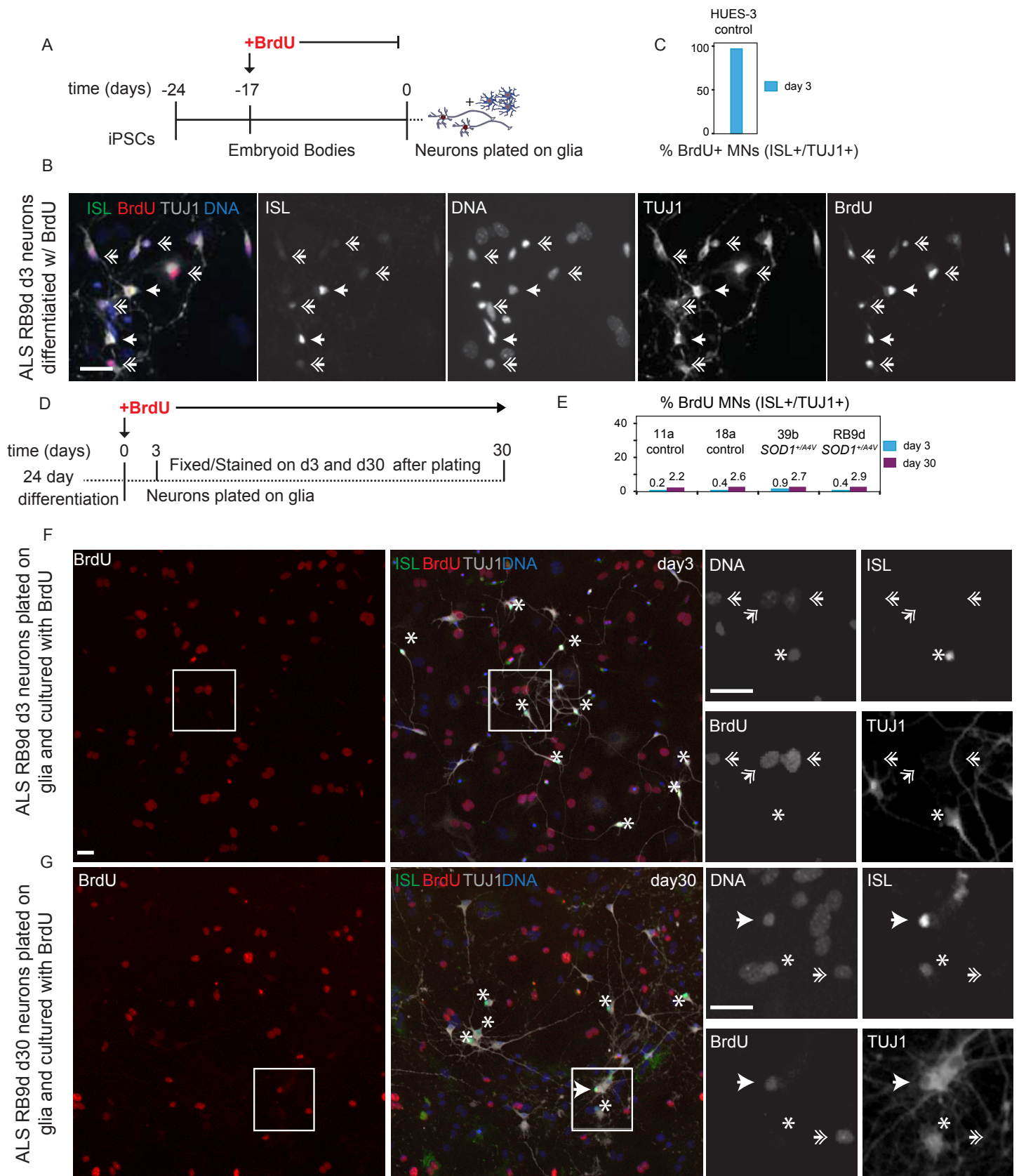
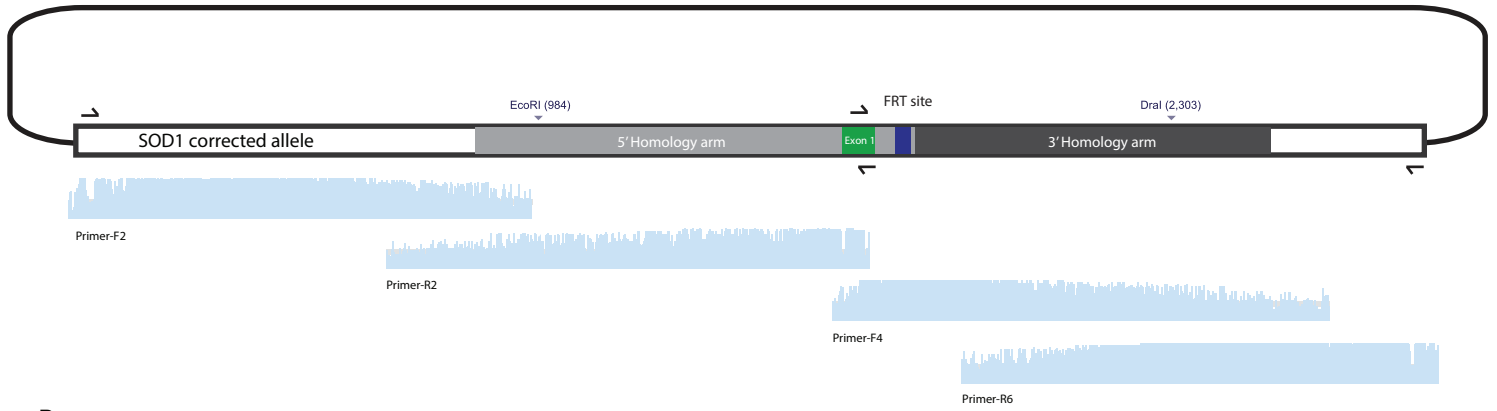


Figure S4, related to Figure 1, Neuronal Proliferation Does not Contribute to the Difference in Motor Neuron Survival Between Control and *SOD1^{+/A4V}* motor neurons. (A-C) Testing the ability of BrdU to label MNs. Differentiation media was supplemented with 1 μ M BrdU between days -17 to 0. Nearly 100% of neurons were labeled by day 3 after dissociation. Importantly the mitotically active, supporting glial cells were never exposed to BrdU in this experiment. **(D-E)** Schematic of experimental strategy to evaluate the level of MN proliferation after dissociation; 1 μ M BrdU was added in plated co-cultures from days 0-30 and percentage of positive cells was analyzed. Between 0.2-0.8% of all MNs incorporate BrdU between days 0-3 while 2-2.8% between days 0-30 across all the iPSC lines. Importantly the mitotically active supporting glial cells were exposed to BrdU in this experiment and many are BrdU+ (large DAPI nuclei). A representative image of BrdU incorporation after the addition of 1 μ M BrdU to dissociated MN cultures after 3 **(F)** and 30 **(G)** days. Top right inserts exhibit an ISL+/BrdU negative MN, bottom inserts exhibit two ISL+ MNs, with only one being positive for BrdU also. Single arrows indicates BrdU+/ISL+ MNs; Double arrows indicate BrdU-/ISL- cells; Asterisks indicate BrdU negative/ISL+ MNs, (scale bar=30 μ m).

A

TOPO plasmid pCR-4



B



C

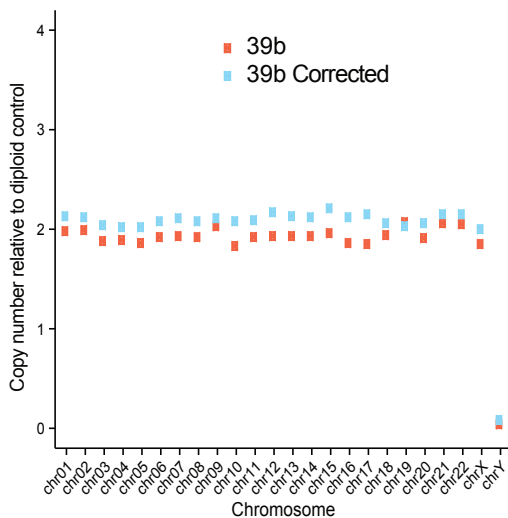


Figure S5, related to Figure 2, Quality Control Assays for the Isogenic Control iPSC line 39b-corrected cell line. (A) In order to confirm proper targeting and correction of the *SOD1*A4V mutant allele, a region of the *SOD1* locus from iPSC line 39b-corrected was PCR-amplified in a single reaction with primers beyond the 5' and 3' homology arms and cloned into a TOPO vector. This was sequenced and compared to the *SOD1* genomic sequence. The FRT footprint is the only site that does not match to the control sequence. **(B)** To evaluate whether large-scale copy number alterations had arisen during gene-targeting of the *SOD1* locus, we measured sequencing depth of coverage across the genome in 10kb bins for the parental 39b and the corrected 39b control line. Sequencing read depth for the two samples closely matched each other throughout the genome. **(C)** To confirm the absence of large-scale copy-number alterations, the Nanoscope nCounter human Karyotype panel was used to measure the genomic content of each cell line across more than 6 loci per chromosome. This data was compared to a reference genome which harbored no duplications or deletions.

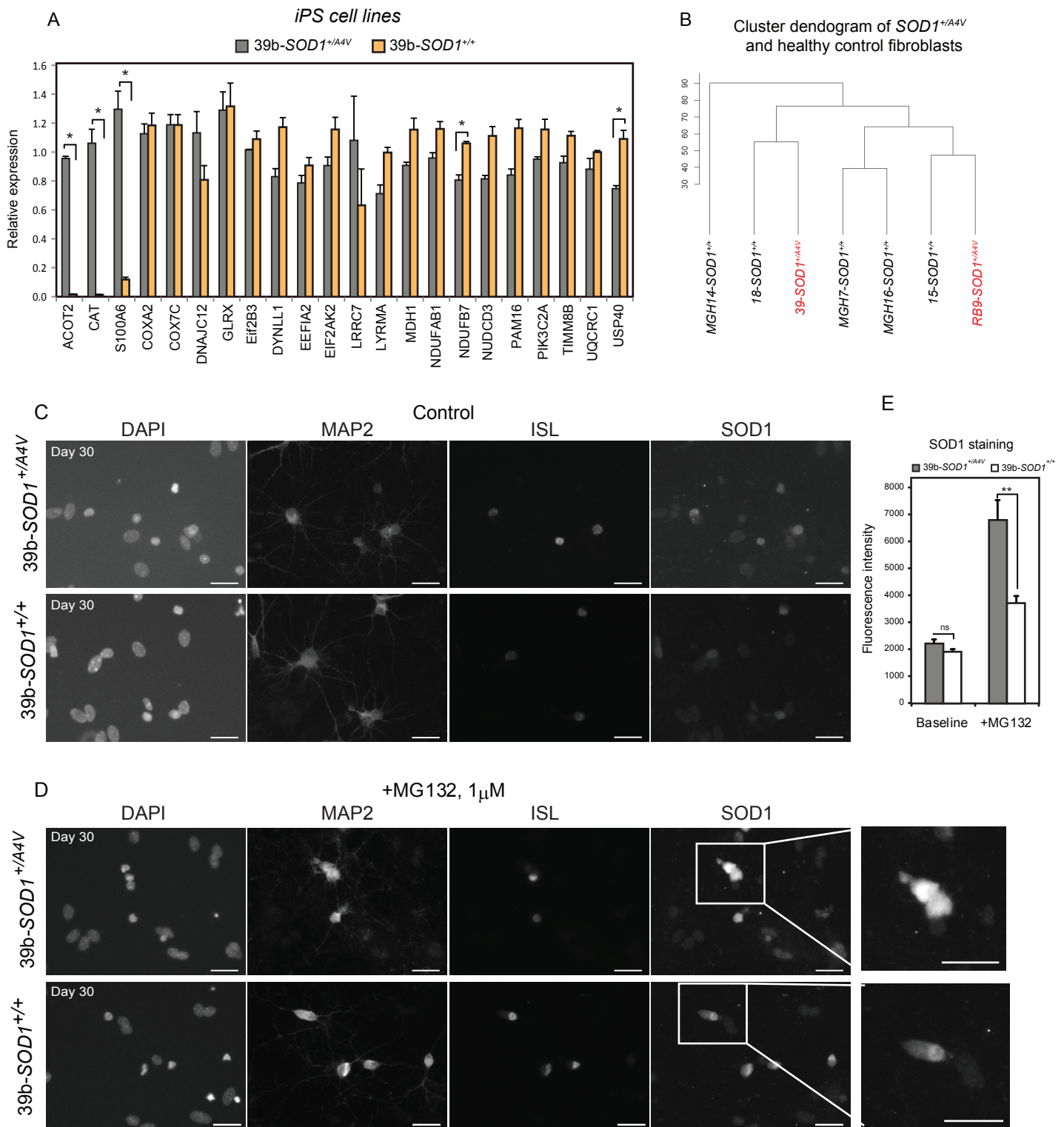


Figure S6, related to Figures 2-3, Differential Gene Expression in non-MNs and SOD1 Protein Accumulation. (A) qRT-PCR analysis in 39b and 39b corrected iPSCs. Genes identified as being differentially regulated as a result of the *SOD1* mutation in *Hb9::RFP* MNs were evaluated in the parental iPSCs. 19% of the genes tested were found as also being significantly different in iPSCs. (B) Cluster dendrogram of RNA sequencing from *SOD1*^{+/A4V} and healthy sex-matched fibroblast samples. The A4V fibroblasts do not segregate from the healthy controls. (C-D) *SOD1*^{+/A4V} MNs accumulate significantly more SOD1 protein after treatment with MG132 (1 μ M, 48hrs) as measured by immunocytochemistry relative to isogenic control MNs. (E) Quantification of the fluorescent intensity of SOD1 protein (n=25, P<0.05).

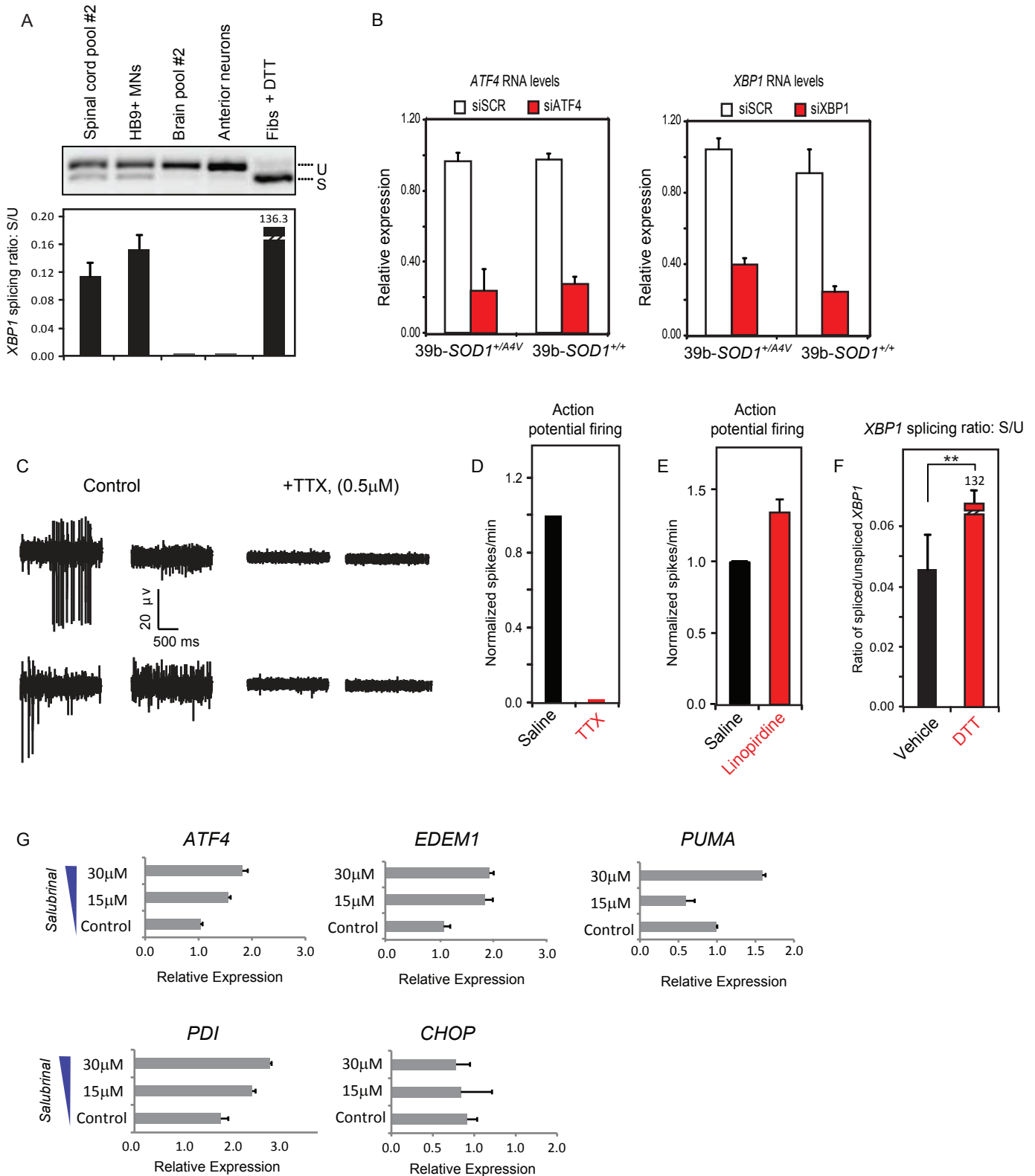


Figure S7, related to Figures 5-6, ER Stress and Electrical Activity are Connected. (A) ES-derived MNs and spinal cord RNA show higher levels of *XBP1* splicing relative to ES-derived anterior neurons and brain RNA. Quantification of gel bands of spliced/unspliced *XBP1* transcript. (B) Knockdown of *XBP1* and *ATF4* by repeated siRNA treatment after 30 days in culture. (C-E) TTX and linopirdine can be used to lower and increase the electrical activity of MNs respectively, as measured by multi-electrode array recording. (F) DTT treatment leads to a strong increase in the levels of *XBP1* splicing. (G) Effects on expression of UPR genes after dosing motor neurons with salubrial.